Weldability of Advanced High-Strength Steel Drawn Arc Stud Welding

Designed experiment is used to statistically quantify fastener welding characteristics of bare boron steel, Usibor®, and HC500C against mild steel

BY C. HSU AND J. MUMAW

ABSTRACT

This paper presents the findings of a weldability study of drawn arc stud welding of various advanced high-strength steels (AHHS) including two grades of boron steel, and one grade of dual-phase steel of various thicknesses and coatings from several automakers, and benchmarked against mild steel. A wide top (or large flange) stud of 6-mm-diameter ISO metric thread (M6) was used in the study. A drawn-arc stud welding process was accomplished by shorting the stud to the workpiece with a pilot current, lifting the stud away from the workpiece to draw a small arc, increasing the current to a high level, holding the stud at the lifted position for a given duration to melt the stud end and the workpiece, and plunging the stud back to the workpiece to complete the weld. Instead of poking for a nine-box weld lobe from trial and error, a robot was used to comb a 3-D weld parameter space of arc current, arc time, and lift height, with parameter grid of 380–1200 welds for each AHHS grade. A design of experiment (DOE) approach maps out the relationship between DOE inputs of control variables, and DOE outputs of weld quality statistically. Objective and subjective weld quality were measured, including destructive conical bend for weld strength, dimple, sag, melt-through, head melting, cracking, excessive expulsion, and backside marking.

Among the 3496 welds visually classified, photographed from both sides and destructively tested, it was found that not all AHHS behave the same in drawn arc welding. Advanced high-strength steel of different types, thicknesses, and coatings exhibited different welding characteristics. Mild steel as a baseline had the classic C or kidney-shaped operating lobe, and the best weldability characterized by the largest lobe size and tolerance to lift. Uncoated boron steel of 1.2- and 1.4-mm thickness had excellent weldability at lower lift, with deteriorating performance at higher lift. It is best welded at hot and fast settings. ArcelorMittal's boron steel Usibor® of 1.4-mm thickness had marginal weldability. It is best welded at slow and cool settings. At 1.0-mm thickness, it could not pull 70% nugget at optimum settings. HC500C of 0.8-mm thickness had unacceptable weldability but shows potential in very hot and fast settings.

Background and Objective

Automakers are considering the use of advanced high-strength steels (AHHS) to reduce vehicle weight and number of parts while improving fuel economy and crash performance (Ref. 1). Depending on the makes and models, there can be dozens to hundreds of studs on each car. Drawn-arc welding using an inverter power source capable of 1800 A of peak current, a servo-electric gun, and pneumatic stud feed, is presently a standard practice in modern automotive plants to weld studs (Ref. 2). Weld process monitoring software is often employed to fingerprint each weld and flag suspect or not-in-order (NIO) welds in production (Ref. 3). The relentless pursuit of quality has driven stud weld defect rate to a 0.8 ppm level (Ref. 4) in some factories employing a Nelson DSP inverter welding machine, servo-electric weld head, and lift-arm stud sorter/feeder, but the use of new materials such as AHHS may adversely affect this weld quality expectation. With intelligent sensing and controls, use of a leg or foot to hold down the workpiece is eliminated from the weld head, and thus a source of downtime because spatter collection at the leg is eliminated. It is important to understand the fastener weldability of various grades of AHHS before it is chosen for a new vehicle body design.

The weldability of AHHS was reported by Emhart Teknologies in a study sponsored by the Auto/Steel Partnership Material Joining Technologies Committee (Ref. 5). Several M6 studs and nuts were welded onto aluminum silicon coated hot-stamped boron steel (Usibor® 1.25 mm) and dual-phase steel (DP980 1.0 mm), along with galvanized mild steel (1.1 mm). Weld nugget > 70% of fusion area without over-melting was used as acceptance criteria for a 120-deg repetitive bend-to-failure test. A "weld lobe development procedure" search routine was used to poke the current-time space in search for acceptable welds (see flowchart in Fig. 4 of Ref. 5). Process robustness was defined by discovering a setting with ±50 A and ±5 ms clearance passing the acceptance criteria, known as a 9-box weld lobe. The search began with an initial set of weld parameters based on experience and adjust the parameters at 50-A, 5-ms increments, and stopped when the 9-box was found. The authors concluded that all the steels studied were weldable with good process robustness.

A study sponsored by BMW Group was conducted to weld chrome-plated M6 paint groove stud with a 13-mm flange to a range of high-strength steels, including DX54D (Z100 coating, 0.66 mm), H300X/DP500 (Z100 and ZE 75/75 BO coating, 0.6 and 0.7 mm), H340XD (Z100 coating, 0.61 mm), H400TD/TRIP700 (Z100 coating, 0.6 mm), and H300X (ZE coating, 0.48 mm) (Ref. 6). The welds were sub-

KEYWORDS

Advanced High-Strength Steel
Drawn Arc Stud Welding
Weldability
Boron Steel
Dual-Phase Steel

C. HSU (chris.hsu@nelsonstud.com) and J. MUMAW are with Nelson Stud Welding, Inc., Elyria, Ohio.

Fig. 1 — Wide-top M6 weld stud.

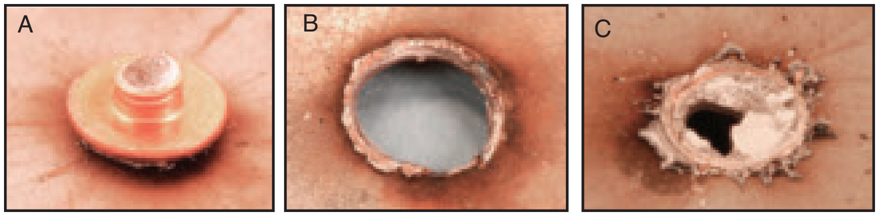

Fig. 2 — Examples of a front-side fracture tensile code after conical bend: A — Code 6: stud shank; B — code 5: 100% hole in base metal; and C — code 2: 30% hole in base metal.

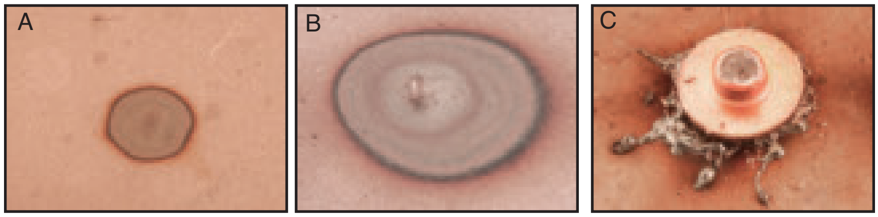

Fig. 3 — Examples of inspection codes: A — Normal heat mark; B — dimple; and C — expulsion.

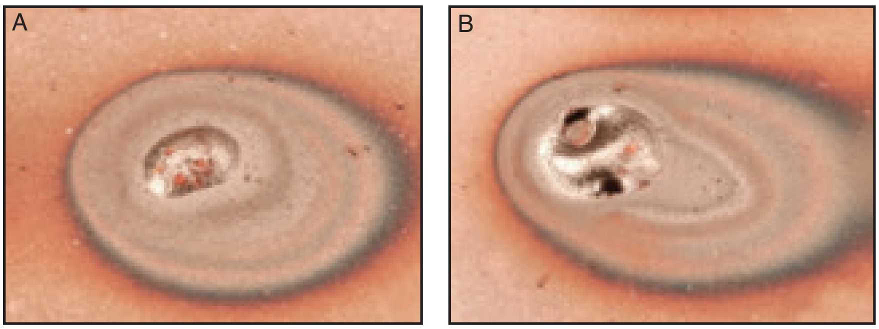

Fig. 4 — Examples of back-side visual inspection codes: A — Melt-through in shiny metal without hole; B — melt-through with hole.

Fig. 5 — NelCell™ DOE setup with legless KSE100 head welding in the flat position.

jected to tensile, torque, and hardness tests. It was concluded that although most welds met the mechanical strength requirement per EN ISO 13918 BMW Group Standard GS 96005, the weldability is a unique characteristic of each material. Each AHHS must be examined separately. For example, TRIP steel has undesirable weld properties.

The drawn arc stud welding process was found to have adequate tensile and fatigue strengths to repair adhesive-bonded joints of DP780 in a study by GM and Shanghai Jiao Tong University (Ref. 7).

Instead of poking around the current-time parameter space, design of experiments (DOE) methodology is demonstrated to better optimize drawn-arc welding process variables and to determine the process viability with statistical confidence and complete understanding of the parameter landscape (Refs. 8, 9). Beside mechanical strength, other subjective quality metrics such as excessive expulsion, backside dimple-shaped deformation, and melt-through with and without creating holes are measured, statistically modeled, and used in conjunction with strength criteria for optimization. Production weld quality statistics at the optimized parameters can be forecast.

The objective of the current study is to employ the DOE tool to quantify the acceptable lobe of welding process variables of selected AHHS grades, and use the AHHS lobes as a relative benchmark against the mild steel lobe.

Experiment and Experimental Procedures

Test Stud

The stud is made of mild steel and has M6 thread, 13-mm flange, 9-mm weld base, copper flash coating, and a length of 25 mm — Fig. 1. This wide top or large flange (known as W-top or LF) stud was chosen to weld all types of base metals in this study because it is very common in North America and Asia, and is gaining popularity in new European car designs.

Base Material

Table 1 — Chemical Composition of Base Material from AHHS Steel Suppliers

Material	Coating	C	Si	Mn	P	S	Al	Ti + Nb	Cr + Mo	C Equi.	Steel Source
Usibor®	Al-Si	0.23	0.26	1.17	0.014	0.001	0.029	0.04	0.00	0.43	Arcelor
Boron	uncoated	0.22	0.26	1.13	0.013	0.003	0.036	0.03	0.15	0.45	Delaco
HC500C	ZE galvanized	≤0.18	≤0.8	≤2.50	≤0.050	<0.01	0.015 to 0.1	≤0.25	≤1.0	—	—

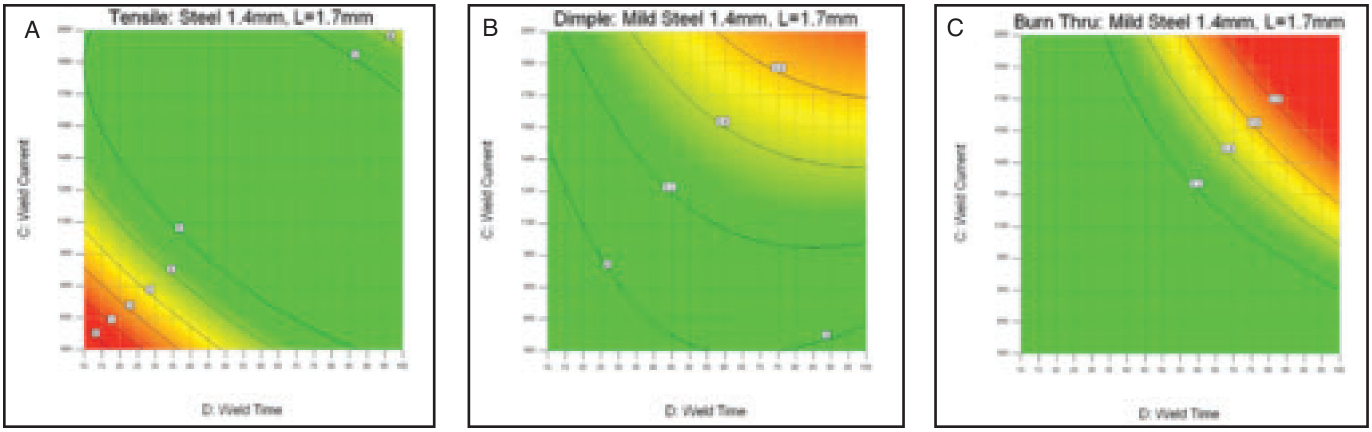

Fig. 6 — Behavior of mild steel 1.4 mm thick at 1.7-mm lift: A — Tensile; B — dimple; C — melt-through.

Table 2 — DOE Weld Parameter Matrix (Each Row is One Grid with a 50-A/5-ms Increment)

Steel	Thickness (mm)	Lift (mm)	Min Current (A)	Max Current (A)	Min Time (ms)	Max Time (ms)	# of Welds in the Grid
Mild Steel	1.4	1.2	1500	2000	10	55	110
Mild Steel	1.4	1.7	500	1450	10	100	380
Mild Steel	1.4	1.7	1500	2000	10	55	110
Mild Steel	1.4	2.5	500	1450	10	100	380
Usibor®	1.0	1.2	300	450	60	110	44
Usibor®	1.0	1.7	300	450	60	110	44
Usibor®	1.4	1.2	300	450	60	110	44
Usibor®	1.4	1.7	500	1450	10	100	380
Usibor®	1.4	1.7	300	450	60	110	44
Usibor®	1.4	2.5	500	1450	10	100	380
Boron	1.2	1.2	1500	2000	10	55	110
Boron	1.2	1.7	1500	2000	10	55	110
Boron	1.4	1.2	1500	2000	10	55	110
Boron	1.4	1.7	500	1450	10	100	380
Boron	1.4	1.7	1500	2000	10	55	110
Boron	1.4	2.5	500	1450	10	100	380
HC500C	0.8	1.7	500	1450	10	100	380

Table 1 shows the chemical composition of base material from AHHS steel suppliers.

Table 3 — Weld Quality Codes

Tensile Code (from conical bend to failure)	Visual Inspection Code
6 — break in stud shank	D — dimple/sag formation but no liquid melt-through
5 — hole is 100% weld base area	B — melt-through with shiny metal
4 — hole is 90–99% of weld base area	H — melt-through with hole
3 — hole is 70–89% of weld base area	M — head melted off
2 — hole is 1–69% of weld base area	C — crack
1 — no hole (fracture in the weld)	E — excessive expulsion or flash
	N — normal/good backside with only heat mark

Experimental Design

The experiment is a response surface model design. In lieu of a conventional two-level D-optimal design with center points and replicates or a five-level central composite design, the authors chose a grid pattern formed mostly by 18 to 19 levels for comparison with the historic lobe data and lobe precision needed in stud welding.

All welds were done in the flat position with direct current electrode negative without shielding gas, as most applications of carbon steel stud welding do not employ protective gas. For each material thickness and lift height, the weld current and weld time were varied by 50-A increments and 5 ms in the range explored (Table 2). The parameter space is normally set to sweep a space bounded by 500- to 1450-A current and 10- to 100-ms time; however, additional spaces (such as hot and fast or cool and slow) were explored when the normal space showed potential in these additional spaces. A total of 3496 studs were robotically welded on a grid pattern.

Weld Quality Assessment

Weld quality was ranked and coded in two scores, tensile code (objective) and visual defect code (subjective). The tensile code is actually the fracture location of a

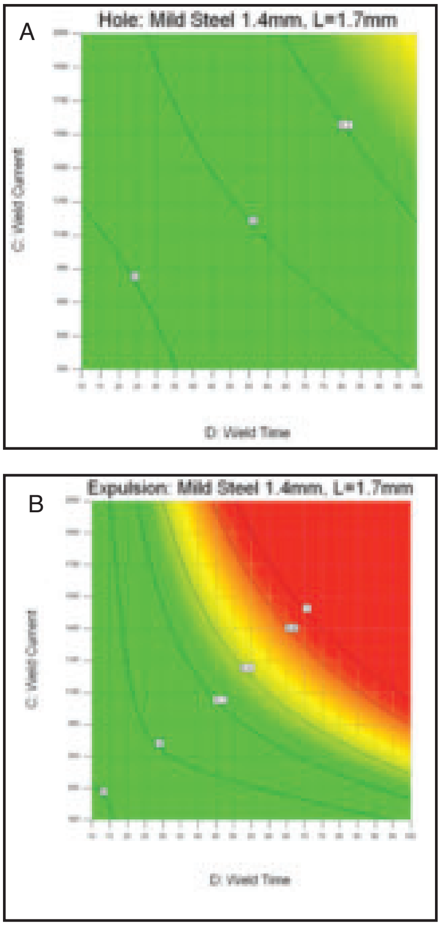

Fig. 7 — Behavior of 1.4-mm-thick mild steel at 1.7-mm lift: A — Hole; B — expulsion.

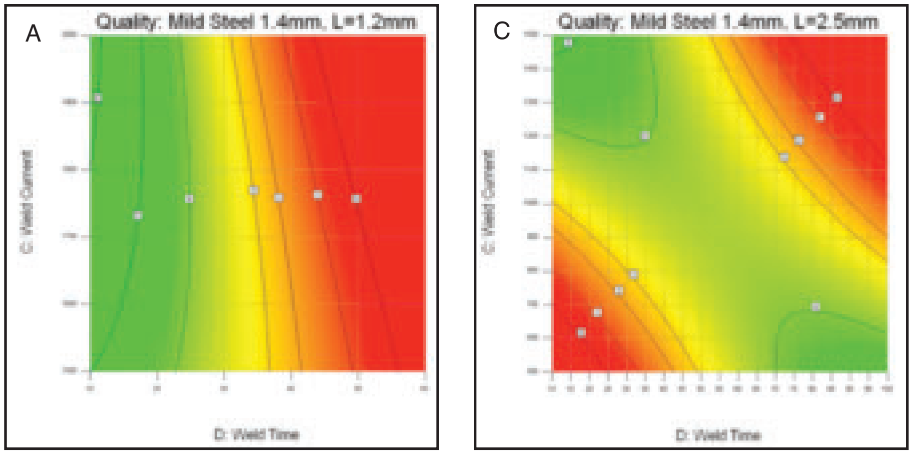

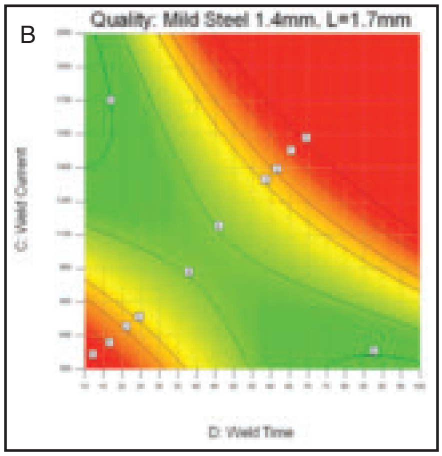

Fig. 8 — Quality code (comprehensive) behavior of mild steel 1.4 mm thick at the following: A — 1.2-mm lift; B — 1.7-mm lift; C — 2.5-mm lift.

Table 4 — DOE Surface Response Models and Their Statistical Significance

Base Material	Result Code	DOE Model Type	F Value	Probability >F	R^2
Mild Steel	Tensile	quadratic	151.2	<0.0001	0.63
	Quality	quadratic	64.3	<0.0001	0.42
	Dimple	quadratic	28.1	<0.0001	0.24
	Melt-through	quadratic	55.1	<0.0001	0.38
	Hole	quadratic	19.1	<0.0001	0.18
	Expulsion	quadratic	191.5	<0.0001	0.69
Usibor®	Tensile	quadratic	253.4	<0.0001	0.67
	Quality	quadratic	14.8	<0.0001	0.20
	Dimple	quadratic	10.5	<0.0001	0.15
	Melt-through	quadratic	55.9	<0.0001	0.48
	Hole	quadratic	32.7	<0.0001	0.35
	Expulsion	quadratic	142.9	<0.0001	0.70
Boron	Tensile	quadratic	88.8	<0.0001	0.53
	Quality	quadratic	88.7	<0.0001	0.53
	Dimple	quadratic	6.9	<0.0001	0.08
	Melt-through	quadratic	92.7	<0.0001	0.54
	Hole	quadratic	11.9	<0.0001	0.13
	Expulsion	quadratic	90.8	<0.0001	0.54
HC500C	Tensile	quadratic	111.6	<0.0001	0.65
	Quality	quadratic	61.3	<0.0001	0.51
	Dimple	quadratic	5.9	<0.0001	0.10
	Melt-through	quadratic	11.7	<0.0001	0.16
	Hole	quadratic	92.0	<0.0001	0.61
	Expulsion	quadratic	7.7	<0.0001	0.11

conical bend test. A tube was inserted onto the welded stud shank and was moved in a circular motion at about 60 deg from the stud axis repeatedly until fracture occurred. This is more advantageous than the planar bend described in Ref. 5 because it has a neutral orientation. A higher tensile code was achieved when the fracture is in the stud shank, or predominantly in the base metal (hence the weld is stronger than the base metal), as shown in Table 3. For example, in Fig. 2C, a hole is torn out in the base metal after the conical bend test. The size of the hole is 30% of the weld area. A tensile code of 2 was thus assigned per Table 3. Visual inspection checks for other irregularities are listed in Table 3, and they are coded 1 as being present, 0 as being absent. Although the visual imperfections are not desirable, they may be acceptable in practical applications. In other words, the visual qualities are highly application specific. For example, the expulsion may not pose dimensional interference and thus may be acceptable if the weld strength is acceptable per the tensile code in Table 3. The output of the DOE will map out the limitations imposed by each visual inspection code. A comprehensive "quality" code is defined below:

Quality Code = Tensile code
(when visual inspection code = N or Normal)

Quality Code = 0
[when visual inspection code = D, B, H, M, C, or E) (M and C are not found in any weld)

The Quality Code is a conservative metric assuming none of the visual impaction is acceptable. This study analyzes weld strength and visual imperfections separately so that automakers can apply to their individual applications, and comprehensively in the form of the Quality Code. Figures 2–4 provide examples of inspection codes.

Welding Equipment

The welding power source used was Nelson's N3 with 2000-A output capacity. Feeder FSE100 was used to feed the stud pneumatically and servo-electric weld head KSE100 was welding in flat position — Fig. 5. The KSE100 can be programmed to precisely position the stud in increments of 0.1 mm during approach, lift, and plunge. The KSE100 is held by a Fanuc 120iB robot in a two-table welding cell. The robot is programmed to automatically weld down a grid of studs with 25-mm spacing between each stud, and either the time is incremented by 5 ms or current is incremented by 50 A from stud to stud.

Results and Discussion

DOE Surface Response Models

Table 4 summarizes the statistical tests of DOE output response models. Each row in Table 4 contains the statistically significant data of each statistical model for each output and steel grade. The weld current and weld time are numerical factors and lift is a categorical factor. The "Probability > F" is a statistical measurement of the likelihood that the observed behavior could have occurred purely as a result of random error. The smaller the value of Probability > F, the greater the significance of the model. All models in Table 4 have a <0.0001 value, meaning highly significant. Statistical models, where the output is a strong function of input factors, tend to have higher R^2 values. All models were chosen to be as simple as possible without transformation while being very significant and passing all statistical diagnostic tests including residuals and Box-Cox plot.

Mild Steel Benchmark

Mild steel (1.4-mm) weld results at 1.7-mm lift are plotted separately in Figs. 6 and 7. These maps are drawn based on statistical models, and use contour lines, or isolines, to plot property codes of equal value, similar to topographic maps with lines to plot elevation. Green is used to denote the highest property code (pass) and red denotes the lowest property code (fail). It can be observed in Fig. 6A that the lower-left corner has insufficient arc energy resulting in a tensile code of less than 3 (or less than 70% fracture in the base metal). In Fig. 6B, the upper-right corner should be avoided if the formation of a dimple is unacceptable. In Fig. 6C, an even greater area of the upper-right corner should be avoided if the precipitation of melt-through with shiny metal (without hole) is not accepted in the application requirement.

Figure 7A paints the entire current-time as a green space without a hole defect. Figure 7B illustrates that an even greater part of the upper-left corner is marked for the presence of expulsion than is Fig. 6C for melt-through.

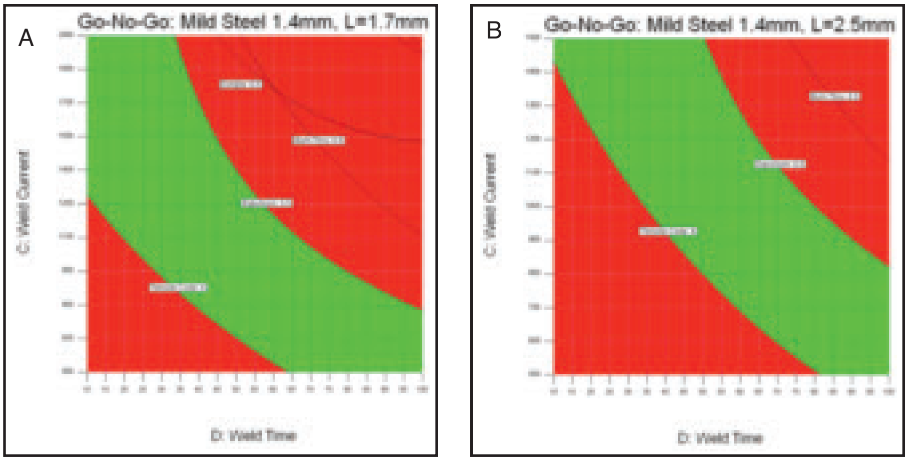

Fig. 9 — Go/no-go operating window of mild steel 1.4 mm thick at the following: A — 1.7-mm lift; B — 2.5-mm lift.

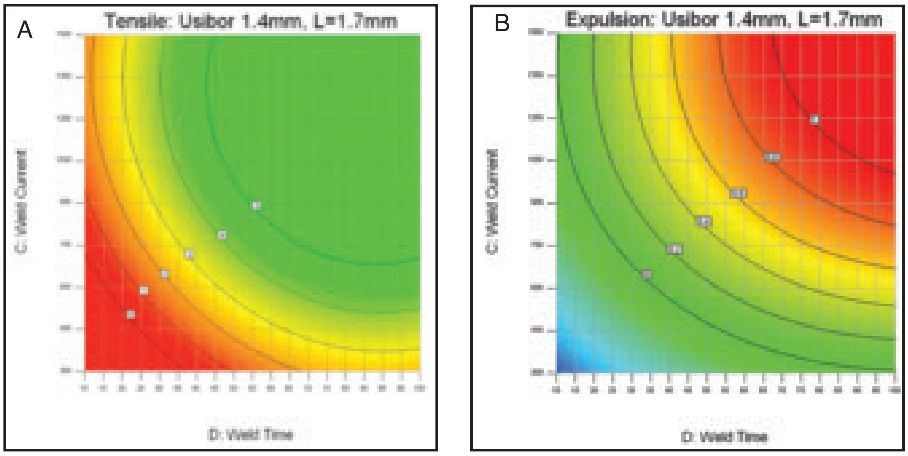

Fig. 10 — A — Tensile; B — expulsion behavior of 1.4-mm-thick Usibor at 1.7-mm lift.

The quality models of mild steel at three lift height settings are compared in Fig. 8. The 2.5-mm lift test is only performed in the hot and fast parameter space. It can be observed that the mild steel has comfortable green zones with a quality code greater than 3 or 4 (over 70% nugget pull in the base metal) in all three lift settings.

To visualize the effect of each quality measure in weld performance, an "operating window analysis" method was used as follows. The pass/fail acceptance criteria were established for each quality response. The map was painted green where all the metrics passed its respective criteria, and red where any metric failed its acceptance criteria. The crisp green lobe (or operating window) based on a set of crisp pass/fail criteria can be used to guide an actual production, e.g., in choosing the operating welding procedure at the center of the green lobe, and in choosing the weld process monitor tolerances to flag suspect welds. The acceptance criteria could vary from application to application, but for the exercise, they were as chosen below:

- Tensile code ≥ 4 (90% fracture in base metal)
- D, B, H, M, C, E < 0.5.

It can be observed in Fig. 9 that the green "go" zone was obtained diagonally from the hot-and-fast setting to the slow-and-cool setting while maintaining proper arc energy delivered to the weld. The low energy corner (lower left) is limited by tensile code (or weld strength), and the high energy corner (upper right) is limited by expulsion. It can be further observed that melt-through is a concern at even higher energy settings; however, it is obscured by the effect of expulsion.

Usibor

The maps of Usibor at 1.7-mm lift reveal the upper-right corner is good for strength, but not good for expulsion — Fig. 10. Other defects are not present. Similar maps are made for the 2.5-mm lift.

The quality code map of both lift settings

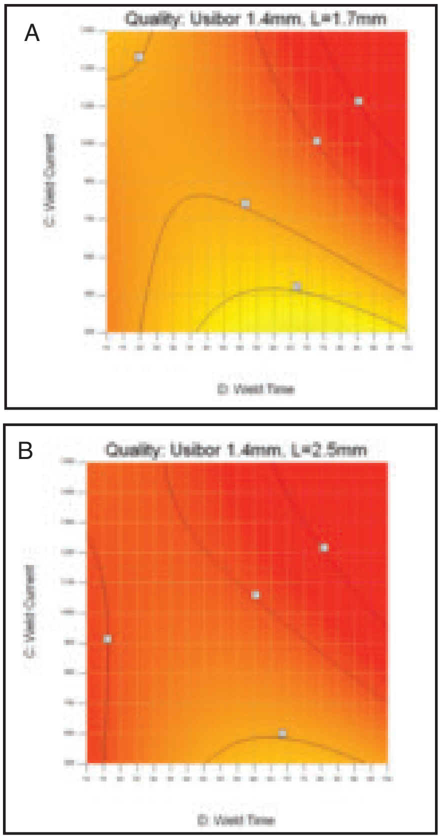

Fig. 11 — Quality code (comprehensive) behavior of 1.4-mm-thick Usibor at the following: A — 1.7-mm lift; B — 2.5-mm lift.

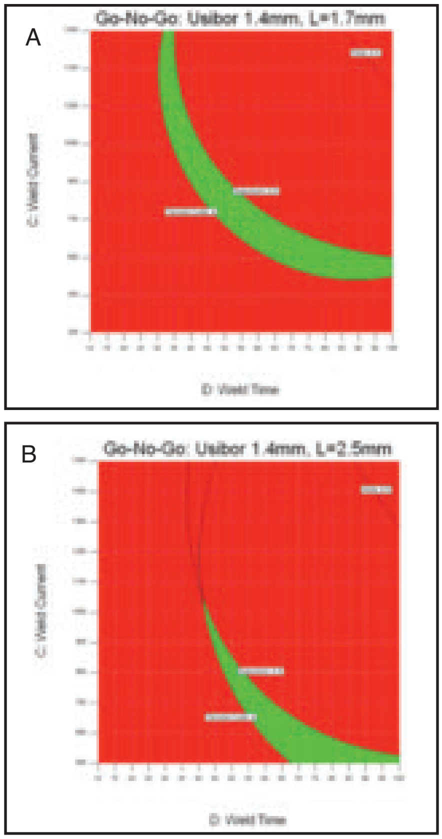

Fig. 12 — Go/no-go operating window of 1.4-mm-thick Usibor at the following: A — 1.7-mm lift; B — 2.5-mm lift.

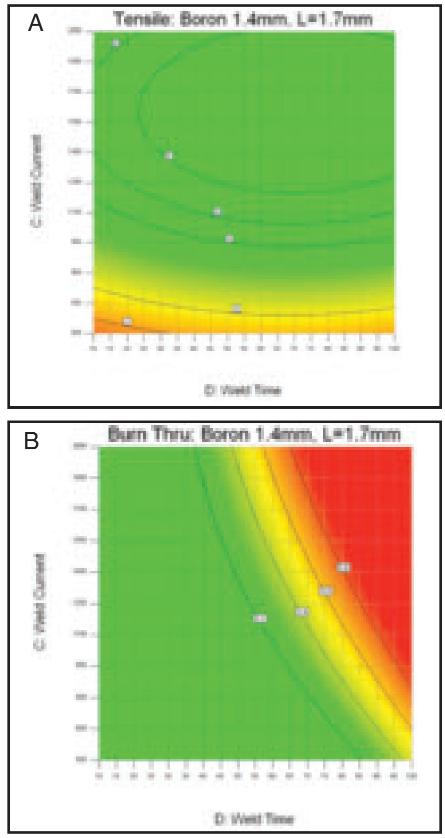

Fig. 13 — Behavior of 1.4-mm-thick boron steel at 1.7-mm lift: A — Tensile; B — melt-through.

is similar, showing poor weldability overall, with better performance at slow-and-cool (lower-right corner) energy settings. Results for 1.0-mm thickness with only slow-and-cool weld tests had worse performance.

The go/no-go maps are exhibited in Fig. 12 for both 1.7- and 2.5-mm lift assuming no visual defect and at least 70% fracture in the base metal. It can be observed that the weldability is marginal at best when compared with mild steel. Of course, if the acceptance criteria are relaxed, the green "go" region would be larger.

For 1.0-mm-thick Usibor plates, a smaller scale sweep focused at slow and cool settings (the most promising) yielded poor strength values with 1.2- and 1.7-mm lift (all below 2, or less than 70% fracture in the base metal).

Boron Steel

The maps of boron at 1.7-mm lift show that it is a very forgiving material with a large green zone for tensile, but the high-energy zone will result in melt-through. Quality code maps of 1.2-mm boron are shown in Fig. 14 where hot-and-fast settings are predicted to work the best.

The quality code maps for 1.4-mm boron steel reveal again that hot-and-fast settings are best suited for this steel. Figure 16 plots the go/no-go windows of 1.4-mm boron steel revealing that it is a quite forgiving steel to weld where the low-energy region is prohibited by poor weld strength while the higher energy settings should be avoided due to first, expulsion and, second, melt-through.

For 1.2-mm-thick boron steel plates, a

Table 5 — Predicted Statistical Behavior of Weld Quality at Optimum Settings

Base Metal		Mild Steel	Mild Steel	Usibor®	Usibor®	Boron	Boron	HC500C
Thickness (mm)		1.4	1.4	1.4	1.4	1.4	1.4	0.8
Lift (mm)		1.7	2.5	1.7	2.5	1.7	2.5	1.7
Current (A)		950	1000	500	300	1556	1450	1450
Time (ms)		55	60	85	90	13	15	10
	Code	5.6	5.4	3.9	3.4	5.7	3.8	2.5
	SE	0.08	0.08	0.14	0.32	0.16	0.22	0.20
Tensile	95% Cl low	5.41	5.21	3.65	2.83	5.42	3.37	2.11
	95% Cl high	5.75	5.53	4.18	4.07	6.03	4.23	2.91
	Code	4.1	3.6	2.2	2.9	6.5	3.7	2.9
	SE	0.14	0.14	0.16	0.38	0.20	0.28	0.21
Quality	95% Cl low	3.78	3.28	1.89	2.11	6.09	3.15	2.54
	95% Cl high	4.35	3.84	2.53	3.60	6.88	4.27	3.36

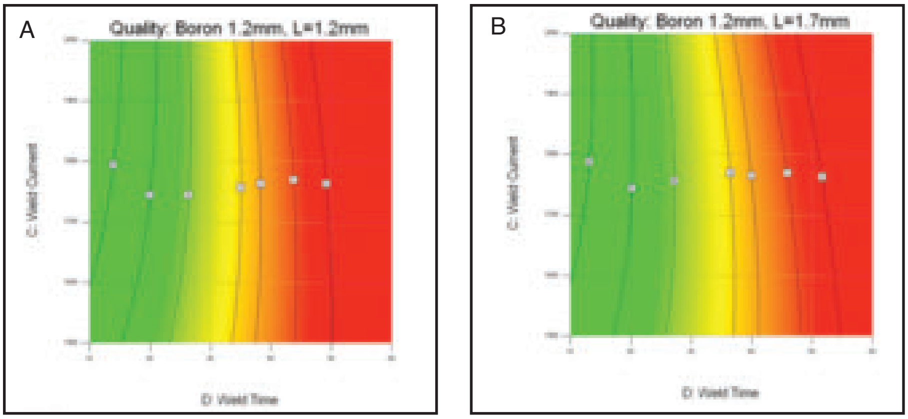

Fig. 14 — Quality code (comprehensive) behavior of 1.2-mm-thick boron steel hot-and-fast settings with the following lift: A — 1.2 mm lift; B — 1.7 mm.

smaller scale sweep focused at hot and fast settings yielded excellent quality values (above 5 and 6).

HC500C

The DOE study of 0.8-mm HC500C reveals a different story in Fig. 17. The tensile map shows only the high-energy settings (upper-right corner) can yield satisfactory strength; however, the same area has a propensity for melt-through hole formation. Poor weldability of HC500C is illustrated, respectively, in the quality code and go/no-go maps — Fig. 18.

It can be argued that the difference in weldability of different steel grades primarily lies in the strength contest between the base sheet metal, the stud shank, and the weld. This is because the acceptance is not the absolute strength, but the assumption that the weld must be relatively stronger than the base metal, as evidenced by tearing a hole in the base metal during destructive testing; or stronger than the stud shank, as evidenced by breaking in the shank. Therefore, base metal strength, thickness, and ductility can influence the fracture location (the weakest link). The weldability is progressively poorer with higher ultimate tensile strength, from mild steel of 440 MPa, to 600-MPa boron steels before hot stamping, to 900-MPa HC500C. In addition, zinc surface coating had a detrimental effect in weld quality when uncoated boron steel was compared with coated Usibor, because it is a contaminant and forms porosity, as well as lowers arc voltage and heat input.

Effect of Arc Energy

Arc energy has a direct impact on the weld strength and visual defects. Too little energy results in insufficient fusion and thus compromises weld strength; too much energy results in dimple and melt-through. Mild steel weld strength expressed in tensile code is plotted in Fig. 19A and the corresponding quality code is plotted in Fig. 19B. It can be observed that there is a window between 44 and 54 Amp*sec where the quality code stays at 6. To match with a given weld size, the required energy can be delivered in the manner of high current and short time ("hot and fast"), or lower current and longer time ("slow and cool"). This simplified analysis collapses the 2-D weld parameter space into one dimension — energy only — without taking into account if the energy is delivered hot and fast, or slow and cool. In other words, the heat loss factor due to conduction, or heat efficiency, was not considered. None of the other AHHS has the degree of robustness of mild steel, i.e., a process that is not affected by the speed of energy delivery, or heat input efficiency.

It can be observed in Figs. 20B and 21B that there is no window of arc energy in which the quality code stays at 6, as in mild steel. It means the energy delivery speed, unlike mild steel, becomes a governing factor when welding these boron steels, coated or uncoated. Very few HC500C welds break in the stud shank seen in Fig. 22A with tensile code 6. Although HC500C can achieve good weld strength by pulling 100% base metal nugget (tensile code 5), the overall quality of the same arc energy is downgraded to zero in Fig. 22B from visual discontinuities rendering it the least weldable steel in this study. Applications less restrictive in these visual attributes will have a better chance of identifying workable arc energy.

Weld Quality Prediction Using Optimum Process Parameters in Production

The statistical behavior of weld quality metrics for a hypothetical production run at optimum weld setting can be predicted from the response surface models, shown in Table 5. SE is mean standard error, and CI is confidence interval of average. Mild steel has high strength and quality values at both low and high lifts, and the most consistent quality values characterized by low standard error and confidence interval. With mild steel base metal as a benchmark, it can be quantitatively predicted that HC500C has the worst weldability followed by Usibor with quality code below 3 (or less than 70% base metal pull). Usibor works best with low current, and HC500C in 0.8 mm thickness works best with hot and fast settings. Boron steel at 1.7-mm lift rivals mild steel for excellence in weldability;

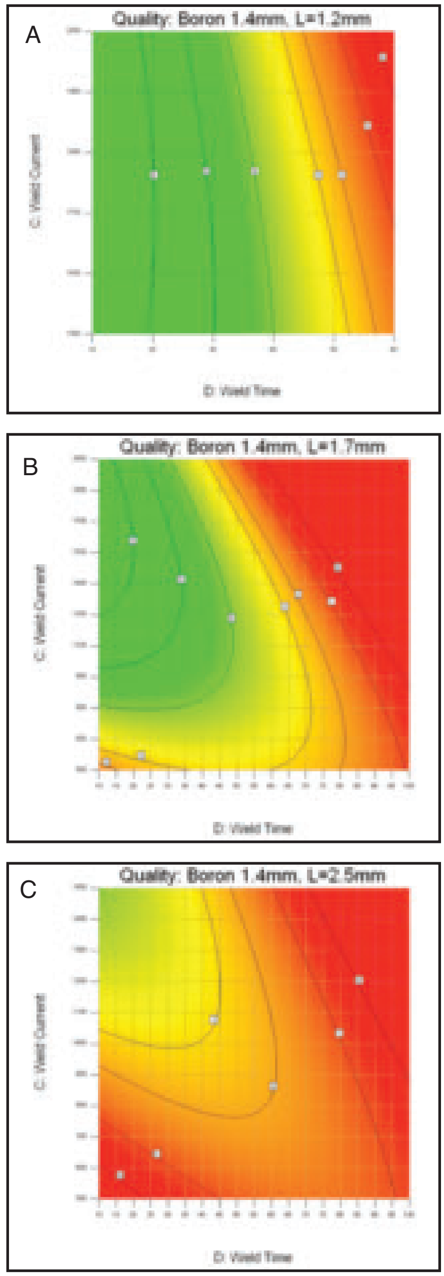

Fig. 15 — Quality code (comprehensive) behavior of 1.4-mm-thick boron steel at the following lifts: A — 1.2 mm; B — 1.7 mm; C — 2.5 mm.

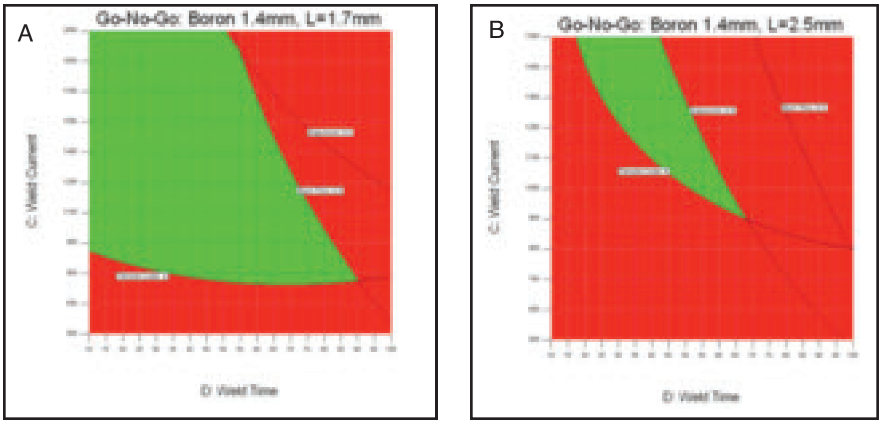

Fig. 16 — Go/no-go operating window of 1.4-mm-thick boron steel at the following lifts: A — 1.7 mm; B — 2.5 mm.

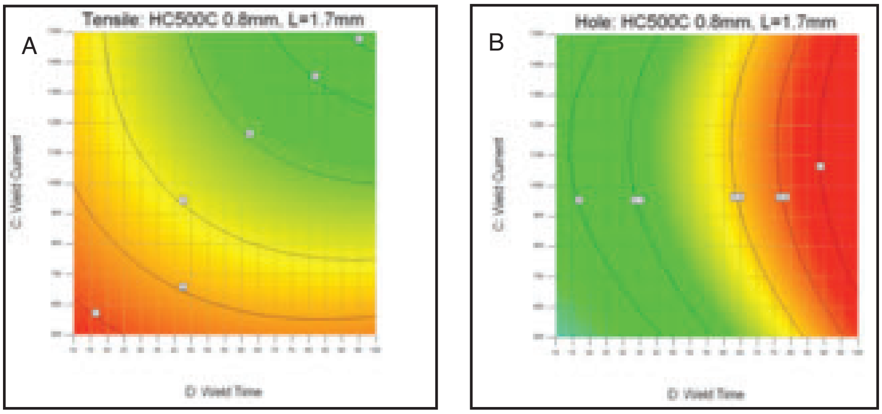

Fig. 17 — Behavior of HC500C at 1.7-mm lift: A — Tensile; B — hole.

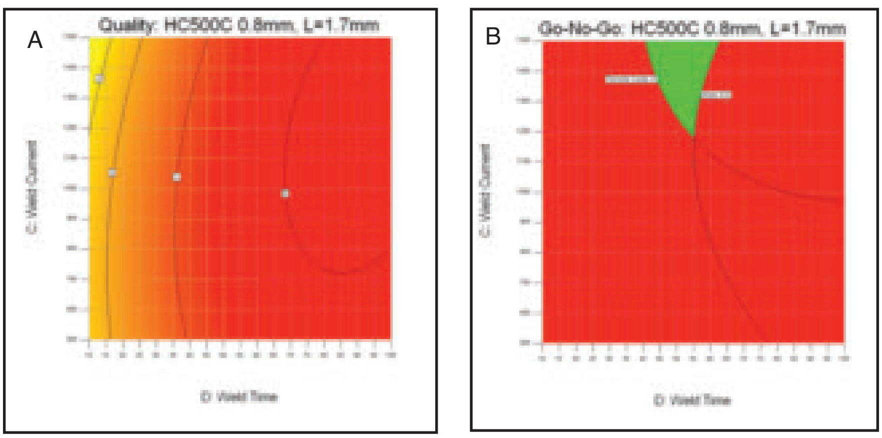

Fig. 18 — HC500C at 1.7-mm lift: A — Quality code map; B — go/no-go map.

however, at 2.5-mm lift, it falls behind mild steel significantly. In other words, boron is not as tolerant as mild steel to actual lift changes in production, e.g., from base sheet metal vibration.

Conclusions

A design of experiment (DOE) was conducted to drawn-arc weld wide-top M6 mild steel studs to several advanced high-strength steel (AHHS) sheets of different thicknesses and surface coatings. Destructive bend fracture behavior and visual defects of Usibor, bare boron steel, and galvanized HC500C are benchmarked against bare mild steel. Surface response statistical models were constructed by analyzing 3496 welds obtained through automated robotic welding to sweep the current-time landscape. It was found that:

1. AHHS weld quality and optimum weld setting varied greatly depending on the steel type, coating, and thickness.
2. Mild steel had the most tolerant operating window in high and low lifts and had the most predictable quality in production.
3. Uncoated boron steel (1.4 mm) in general had excellent weldability and was best welded at hot and fast settings. There is a need to watch out for weaker weld strength at higher lift settings and melt-through at higher weld energy. Thinner, uncoated boron steel with a thickness of 1.2 mm also yielded excellent weldability.
4. Usibor (1.4 mm) had poorer weldability than uncoated boron steel and was best welded at slow and cool settings. In particular, it had a narrower operating window for achieving good weld strength at the nominal 1.7-mm lift in comparison with uncoated boron. Usibor with 1.0-mm thickness could not pull more than a 70% nugget in the base metal.
5. HC500C (0.8 mm) had the worst weldability because there is little common ground of parameter real estate between weld strength and avoiding melt-through hole defect formation. A hot and fast setting holds the most promise for finding this common ground.

These findings were based on lab conditions to study carefully controlled process factors while suppressing other "noise" factors. In a production environment, there are many factors that can affect the weld quality that were not studied in this DOE. These factors include ground location, arc blow, polarity, workpiece vibration, stud feeding, handling and positioning, chuck deterioration, weld cable deterioration, part surface contamination, etc. Automakers may have different mechanical testing acceptance criteria and assign different importance to other subjective visual defects and exudation of the welding process. This can result in new optimization of process variables.

Acknowledgments

The authors wish to thank the BMW Group and Ford Motor Co. for their support of this research.

References

1. Wagoner, R. H. 2006. Advanced High Strength Steel Workshop Final Report, Arlington, Va., October 22, 23.
2. Hsu, C., et al. 2007. Portable and intelligent stud welding inverter for automotive and sheet metal fabrication. *Robotic Welding, Intelligence and Automation*, Springer Berlin/Heidelberg, ISSN 0170-8643, September, pp. 367–374.
3. Champney, C., and Hsu, C. 2009. Shear

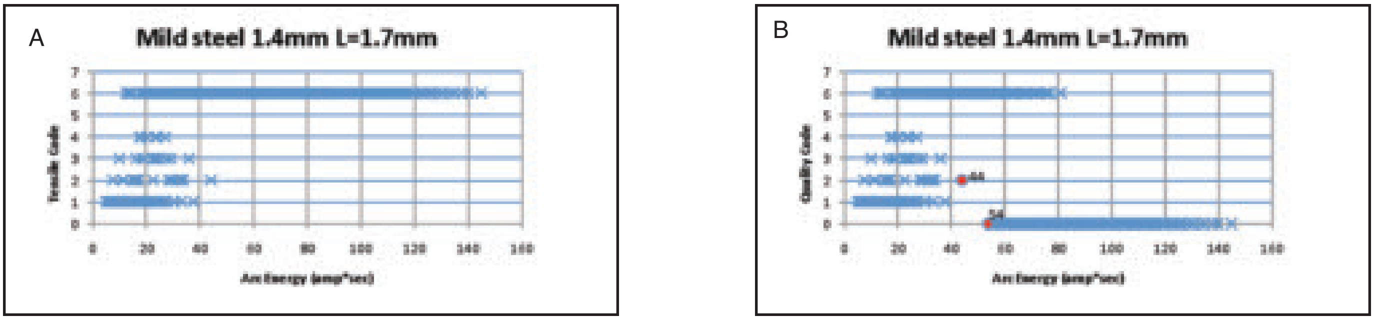

Fig. 19 — Effect of arc energy on mild steel: A — Tensile code; B — quality code.

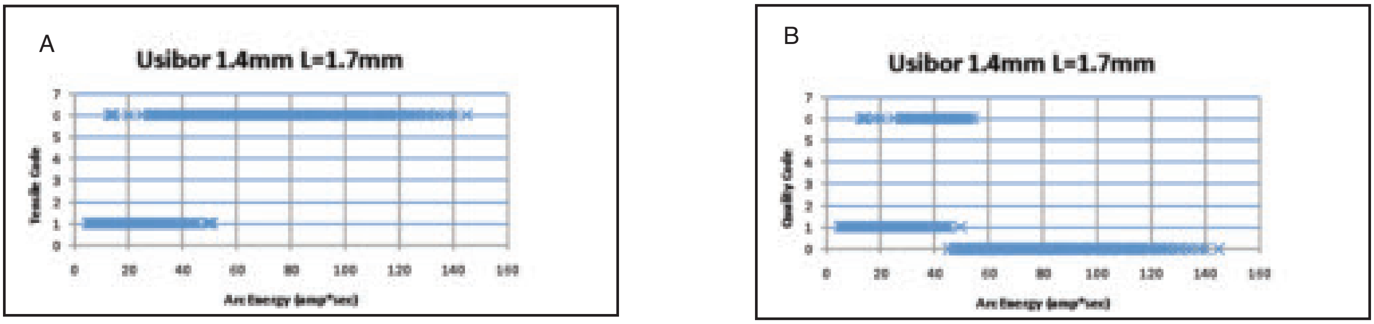

Fig. 20 — Effect of arc energy on Usibor: A — Tensile code; B — quality code.

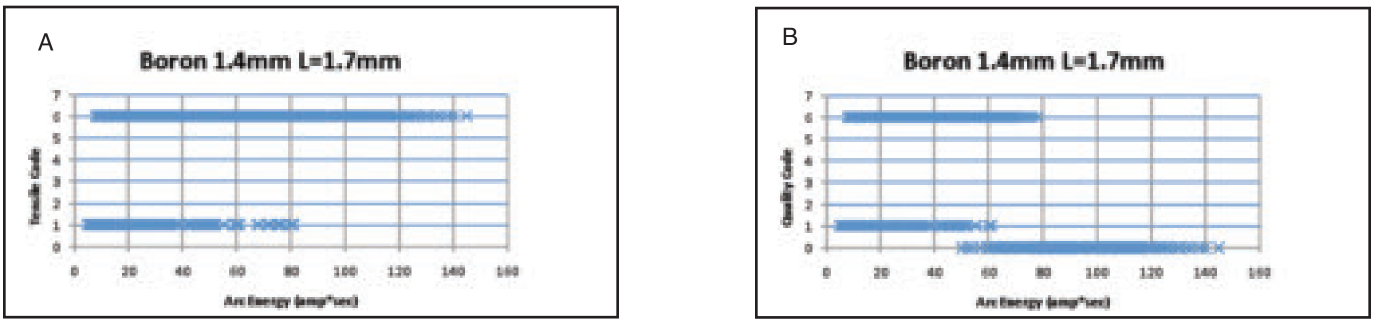

Fig. 21 — Effect of arc energy on boron steel: A — Tensile code; B — quality code.

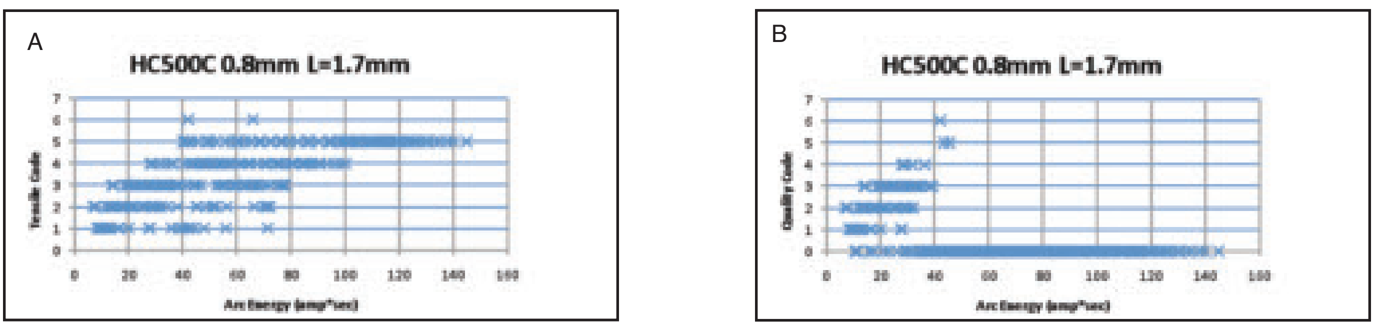

Fig. 22 — Effect of arc energy on HC500C: A — Tensile code; B — quality code.

connection in bridges using studs with precast panel decks. 2009 World Steel Bridge Symposium, AISC/NSBA.

4. BMW internal weld quality production reports, April 2008.

5. Ramasamy, S., Chinoski, R., and Patel, B. 2006. Weld lobe development and assessment of weldability of common automotive fasteners using drawn arc welding process. Report for Auto Steel Partnership.

6. Zganiatz, J. 2005. Großflansch-Bolzenschweißen nach dem Hubzündungsverfahren — Qualifizierung, Verfahrensgrenzen und Auswirkungen bei Produktionseinsatz, Matrikelnummer: 200027119, April.

7. Yang, H. J., et al. 2010. Method for repairing of adhesive-bonded steel. *Materials & Design*, Volume 31, Issue 1, pp. 260–266.

8. Hsu, C., Mumaw, J., Thomas, J., and Maria, P. 2008. Robotic stud welding process optimization with designed experiment. *Welding Journal* 87(10): 265-s to 272-s.

9. Ramasamy, S., Gould, J., and Workman, D. 2002. Design-of-experiments study to examine the effect of polarity on stud welding. *Welding Journal* 81(2): 19-s to 26-s.